AD-A128 353 MECHANICS AND PRACTICE (SELECTED ARTICLES)(U) FOREIGN TECHNOLOGY DIV WRIGHT-PATTERSON AFB OH Z FU ET AL. 28 MAR 83 FTD-ID(RS)T-0016-83 1/1

UNCLASSIFIED F/G 20/4 NL

END
DATE
FILMED
6 83
DTIC

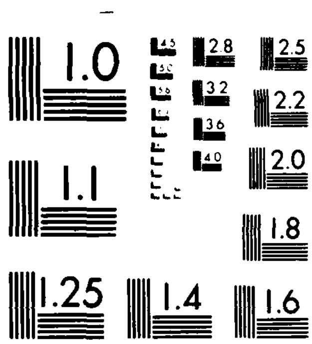
1.0
1.1
1.25
1.4
1.6
1.8
2.0
2.2
2.5
2.8
3.2
3.6
4.0

2

FTD-ID(RS)T-0016-83

AD A128353

FOREIGN TECHNOLOGY DIVISION

AIR FORCE SYSTEMS COMMAND

MECHANICS AND PRACTICE

(Selected Articles)

FOREIGN TECHNOLOGY DIVISION

DTIC
SELECTED
MAY 19 1983
S E D

DTIC FILE COPY

Approved for public release;
distribution unlimited.

83 05 19 026

FTD-ID(RS)T-0016-83

EDITED TRANSLATION

FTD-ID(RS)T-0016-83 28 March 1983

MICROFICHE NR: FTD-83-C-000504

MECHANICS AND PRACTICE (Selected Articles)

English pages: 41

Source: Lixue yu Shijian, Vol. 4, Nr. 3, 1982, pp. 19-23; 39-43; 78-81

Country of origin: China
Translated by: SCITRAN
F33657-81-D-0263
Requester: FTD/TQTA
Approved for public release; distribution unlimited.

PREPARED BY:

TRANSLATION DIVISION
FOREIGN TECHNOLOGY DIVISION
WP-AFB, OHIO.

TABLE OF CONTENTS

GRAPHICS DISCLAIMER

All figures, graphics, tables, equations, etc. merged into this translation were extracted from the best quality copy available.

SEVERAL PROBLEMS IN THE DESIGN OF ENVIRONMENTAL WIND TUNNELS*

Fu Zhifu

Environmental Group, Department of Mechanics
Beijing University

I. INTRODUCTION

For many years, the research and development of new aircraft has been the main promotional force in the development history of wind tunnels. People already overcame the sound barrier in the 40's and the heat barrier in the 50's. Furthermore, we are satisfactorily solving the problems of re-entry into the atmosphere of manned space-craft. Despite these advances, there are still many problems in the subsonic region to be resolved urgently by workers in aerodynamics.

Since the late 50's and early 60's, problems such as the simulation of atmospheric motion, the study of turbulence diffusion and the wind load and wind flutter of high rise buildings and structures have presented new requirements for the development of low velocity wind tunnel techniques. Between 1945-1955, Michigan University in the U.S. modified the length of a low velocity wind tunnel with an experimental cross-section of 2.4m x 1.5 m, from 4.6 to 10.7 m to adapt to non-aeronautical applications. At Colorado State University in the U.S., Cermak,et al began the development of a micrometeorological wind tunnel in 1958. In the experimental section of their wind tunnel, there is a base plate which can be heated or cooled. In the return flow section, there is a snake shaped tube for heating or cooling the ambient temperature. The sectional area in the test section is 1.8x x 1.8 and the length is 30 m. The top plate in the test section is adjustable. Its wind velocity is appromately 0.1 m/s-37 m/s. It can naturally form an atmospheric boundary layer 1m thick. It is also capable of simulating the temperature layer structure in various states. The Marseille Turbulence Statistical Research Institute in France built a wind water channel in 1970. The length of the test section is 40 m.. The cross-

*An Weipo, Yi Jiefen, Wang Xiying, Ye Wenhu and Fu Zhifu were involved in the literature search and review. It was authored by Fu Zhifu.

sectional dimensions are 3.2 m x 1.45 m. The wind velocity is 0.5 m/s to 14 m/s. The flow velocity of the water channel is 0.01 m/s - 0.1 m/s. The water channel is 2.6 m wide and 0.75 m in depth. In this wind water channel, it is possible to simulate the turbulence boundary layer. It is also possible to control the velocity, temperature and humidity of the gas. Furthermore, it is possible to control the velocity, temperature and chemical composition of the water. In the middle 70's in England, Oxford University was constructing a new environmental wind tunnel. Its experimental cross-section is 4 m x 2 m. In Japan, many environmental wind tunnels were built since the 70's. The newly constructed wind tunnel by the Japanese Pollution Research Institute, with an experimental cross-section of 3 m x 2 m and a length of 24 m, is a typical one. This is an environmental wind tunnel with more or less the complete features required. In summary, the development of environmental wind tunnels is still in progress internationally. The experimental techniques are also revised and gradually perfected day by day.

II. THE CHARACTERISTICS OF AN ENVIRONMENTAL WIND TUNNEL

A low velocity wind tunnel for aeronautical application usually
requires low turbulence, i.e., $\varepsilon \leqslant 0.1\%$, . Therefore, the contraction 19
ratio is frequently above 6:1. The flow in the test section is a steady uniform flow. The test section may be very short. It is approximately 1.5-2.5 times the larger dimension in the cross-section. For certain special tests such as the drop test, of course, a longer experimental section is needed.

However, the problem to be studied by us here is the simulation of the environmental fluid dynamics problem in the atmospheric boundary layer. It can be imagined that the flow conditions to be simulated in an environmental wind tunnel are far more complicated than that of an aeronautical wind tunnel where only a uniform flow is required. A comparatively complete atmospheric simulation device should be capable of simulating the following aspects, i.e., the atmospheric turbulence structure, the various velocity sections under different geomorphological conditions, the temperature gradients under various stable conditions, the air humidity with a certain range, the interaction between the water-gas interface, and the variation of wind direction with altitude.

Most environmental wind tunnels can only simulate the contents of the first four items. For example, the micro-meteorological wind tunnel at Colorado State University in the U.S. can be considered as a wind tunnel with comparatively complete features. However, it is only capable of completing the simulation of the first four items. The wind water channel at the Turbulence Statistic Research Institute in Marseille, France, can simulate the first five items. As for the simulation of wind direction variation with altitude, usually, in the surface layer (below 100 m) near the ground and for a short distance (within 5 km) the effect of Kerr's force can be neglected. Of course, this effect can be corrected using a numerical method. However, the wind tunnel equipment itself cannot simulate the variation of wind direction with altitude at the present time. Currently, when it is required to study the turbulence diffusion law of a large geomorphological region at a high altitude from ground (above 100 m), then it is necessary to use a rotary device to complement the simulation experiment. This type of rotary was designed for the purpose of studying the unstable Ekmand boundary layer.

An environmental wind tunnel usually requires a turbulent factor of $\varepsilon \sim 1\%$. From the point of view of the contraction ratio of the 20
wind tunnel, it is seldom more than 6:1. Of course, it would be better if the conditions allow for the wind tunnel to be designed to reach low turbulence $(<0.1\%)$. In the simulated experimental process, it is also possible to artificially change the turbulence. This approach is more active. However, it is not easy to realize structurally, especially in a large wind tunnel.

With regard to the simulation of velocity section in an environmental wind tunnel, the most effective way is to use a long test section. Taking the micro-meteorological wind tunnel at Colorado State University and the wind tunnel with a test section of 2.4 m x (1.8-2.4)m x 30 m at West Ontario University in Canada as examples, the test section is about 30 m long. J. E. Cermak and A. G. Davenport both believed that for the balanced development of the velocity section and temperature section turbulence characteristics, it must rely on the natural lengthening of the boundary layer. This must require a long test section. The external boundary layer is completely developed at about 10 m from the inlet of the test section. The vertical cross-section of its average velocity, turbulence strength and Reynolds shearing stress begin to be similar to the natural conditions. Further downstream, along with the thickening of the boundary layer, the velocity section shows a similar distribution in proportion. Approximately after 24 m, the thickness of the naturally formed atmospheric boundary layer can reach about 1 m. Generally speaking, as long as the coarse elements are matched properly, then the naturally formed boundary layer turbulent structure agrees with the natural conditions.

Another way to simulate the velocity section in the atmospheric boundary layer is artificial formation. This involves the use of an artificial method to accomplish it in a comparatively shorter test section (the length at least cannot be less than 6 times the smallest dimension in the cross-section). Strom at New York University believed that in a short test section if measures are taken to increase the resistance by layer at the inlet and outlet, it may be possible to form the required velocity section. Of course, in the turbulence structure aspect, it is also possible to use a trial composition method to make it agree with or apprxoimately similar to the natural conditions. There are many ways to artificially form the atmospheric boundary layer. They are discussed separately as follows:

1. Cascade and gradient cascade. By placing cylindrical rods parallell from the base plate to the top plate across the inlet of the test section, the resistance between layers is made different by the dense to loose spacing between the rods to promote the formation of a velocity section with a gradient.

2. Curved mesh. A curved mesh is secured on the bottom plate at the inlet of the test section to vary the resistance of the flow

at various layers. When the gas flow passes through the mesh and the coarse element, a velocity section with a gradient is generated.

3. A whirlpool generator. An artificially thickened boundary layer is obtained by using a 1/4 elliptical plate (or a sharp tower), a wall type barrier plate and a coarse element. By using this method, an atmospheric boundary layer thickness equivalent to the height of the 1/4 elliptical plate can be obtained at a distance approximately three to four times the height downstream from the plate.

4. A perforated plate velocity vehicle. The lateral adjustment of the open and shut ratio of uniformly perforated plates at various layers is used to create a varying resistance between layers to cause the formation of various velocity sections. In th 3 m x 24 m wind tunnel at the Japanese Pollution Research Institute, this device is used together with a manual weight adjustment fish scale plate coarse element to form the mechanism for the formation of the artificial boundary layer. Because this method involves the adjustment of the open to shut ratios of the plate at various layers to obtain the various velocity sections correspondingly, it is very flexible and dynamic. However, this uniformly layered method most frequently cannot provide the satisfactory velocity gradient in the lower part of the velocity section. This may be due to the fact that, near the bottom plate, the velocity variation is very large corresponding to a slight variation in height. With regard to this point, it is necessary to fine tune the velocity section near the bottom plate in order to make it agree better with the actual situation. This can be accomplished by added various coarse elements at the layer plates near the bottom plate for adjustment. It is also possible to divide the layers more densely near the bottom plate. It can be made less dense from the bottom up so that the turbulent dimension and strength can be controlled.

5. The injection technique. This is a method to increase the thickness of the boundary layer by injecting air from the base plate upward through many slender holes in front of the inlet of the test section. When the injection velocity is sufficient, the boundary layer can be thickened by 3-4 times as compared to the natural growth

condition. If various coarse elements are matched, then not only the boundary layer thickness will be increased but also the turbulent strength will be intensified. Equilibrium can be reached at a very short distance away from the injection area. Another method is the reverse injection technique. This is to place a tube at the inlet of the exerimental section. The tube was punched to form many holes (in a row). A fine tuned regulating valve is used to control the injection velocity of the gas flow. The injection direction may be vertically upward. It may also be inclined forward or backward $(-20^\circ < \theta < 20^\circ)$. 21
Different resistances can be created between the vertical layers based on the strength of the injected gas flow. If this method can be matched properly with various coarse elements, it is possible to form the velocity sections and turbulent structures which agree with the natural situations. This is a comparatively hopeful artificial boundary layer function method which has been developed in recent years.

With regard to the problem of temperature boundary layer formation, it is similarly divided into two types, i.e., the natural temperature boundary layer formation method and the artificial temperature boundary layer formation method. As for the naturally formed temperature boundary layer, such as the one in the micro-meteorological wind tunnel at Colorado State University, a snake-shaped tube heat exchange is placed at the third turn of the wind tunnel to create an ambient temperature of 5°C-95°C. A cooling and heating plate can be added to the bottom plate at approximately 12 m downstream from the inlet of the experimental section. Its temperature range is 5°C-200°C. If the temperature layer structure of a stable state is to be simulated, the bottom plate is cooled and the environment is heated. When the heated ambient gas flow comes in contact with the cooled bottom plate, because the top is hot and the bottom is cold, a gradual convection heat exchange is carried out. The temperature boundary layer is naturally formed and developed. At approximately 24 m downstream from the inlet of the experimental section, a temperature boundary layer of more or less the same thickness as that of the velocity boundary layer can be obtained. If the temperature layer structure of an unstable state is desired, then the situation is reversed. At this time, the ambient temperature has to be cooled down and the bottom plate must be heated. When the ambient and the base plate are neither heated nor cooled, it is the neutral condition. For a wind tunnel of this type, thermal insulation measures must be taken for the tunnel structure itself in order to make the heat loss to be less than 5% of the total heat. The side walls and top plate in the test section are made of a plywood structure. The surface is double coated with an aluminum powder paint. However, the heating and cooling base plate is made of a copper or aluminum plate in order to conduct heat quickly. The glass windows on the sides and at the top are double-walled. Its purpose is also to insulate the heat. As for the artificially formed temperature boundary layer, it is much simpler. For example, in the wind tunnel at Michigan University in the U. S. (2.44 m x 1.52 m x 10.7 m), electrically heated rods are placed at the inlet of the test section at different intervals. These electrically heated rods at various levels are controlled by imposing different voltages to control the temperatures at various layers. This type of mechanism can simultaneously form an artificial velocity boundary layer and temperature boundary layer. Of course, in some wind tunnel experiments, the base plate in the test section will have to be heated or cooled, such as the wind tunnel at New York University (2.14 m x 1.07 m x 12.2 m).

The 3 m x 2 m x 24 m circular environmental wind tunnel at the Japanese Pollution Research Institute has its unique characteristics in the formation of a temperature boundary layer. In addition to the installation of the snake-shaped tube for heating and cooling the ambient temperature at the third turn, the base plate is a temperature vehicle and a velocity vehicle placed at the inlet of the test section. The so-called temperature vehicle is an electrically heated rod divided into many layers which corresponds to the layering of velocity by using the plate with holes. This kind of heating method is actually a combination of the natural formation method and the artificial formation method. It is mainly a naturally formed boundary layer which is assisted by the artificial temperature boundary layer method. By adopting this kind of temperature adjustment, it is possible to obtain the various forms of temperature sections, including the temperature inversion layer structure with a layer of "cover" on top. With regard to the simulation of the temperature layer structure, it is comparatively complete and flexible.

The experimental study of agricultural meteorology and evaporation as well as the study of the energy exchange mechanism between the atmosphere and the ocean require the simulation of atmospheric humidity in the wind tunnel. For example, the micro-meteorological wind tunnel at Colorado State University in the U.S. is equipped with a gas spraying system in the return channel. It was installed downstream from the heat exchanger which is in front of the third turn. Its relative humidity can be controlled within 20-80%. In addition, the Marseille Turbulence Statistic Research Institute in France has a wind water channel which is also equipped with a humidity formation device. The relative humidity at the inlet of the test section can be maintained at 60-100%. This wind water channel can be used to study the mechanisms of mass, momentum and energy transfers between the atmosphere and the ocean surface on a small scale.

When the gas flows along the test section of the environmental wind tunnel, its boundary layer gradually thickens. Consequently, the effective area of the test section is reduced. Under low velocity conditions, the velocity will increase and the local static pressure will be reduced to produce an axial pressure gradient. In the model testing zone, it is not allowed to have an axial pressure gradient. In order to effectively elimnate the axial pressure gradient, the test section in an ordinary aeronautical wind tunnel is comparatively short. The wind velocity used in model testing is comparatively fixed. Hence, a fixed diffusion angle of 0.5° is used to solve this problem. For a wind tunnel with tangential angular fillings (usually it is a short experimental section wind tunnel), the invariant static pressure value can be obtained by replacing the fillings. However, under the conditions of an environmental wind tunnel, because the test section is long and the experimental wind velocity range is wider (0.1 m/s-10 m/s or 0.1 m/s-30 m/s), it is impractical to use a fixed adjustable angle method or a modified tangential angular filling method. Therefore, under most conditions of an environmental wind tunnel, an adjustable top plate method is used to solve the problem. It is used to adjust the height of the top plate based on the wind velocity to make the axial pressure gradient approach zero.

Because along the entire test section length the top plate must be adjustable, therefore, a secondary flow will be created at the four corners of the usual test cross-section. Consequently, the test zone is effectively decreased. The way to eliminate the secondary flow is to shave the angles at the four corners of the rectangular cross-section. However, it is not easy to treat with the adjustable top plate structure. Therefore, it will have to be solved by widening the experimental segment.

III. SEVERAL PROBLEMS TO BE AWARE OF IN THE DESIGN OF ENVIRONMENTAL WIND TUNNELS

In the design of environmental wind tunnels, we have to consider two questions: One is to know what kind of experiments are to be conducted. The other is to know what kind of a wind tunnel is required to carry out these experiments; which is to determine the cross-sectional dimension and shape of the experiment segment as well as the required wind velocity. Based on these requirements, the operating power required is determined and the entire design plan is also roughly decided.

The problems we are going to discuss are limited to the environmental fluid dynamics problems such as the diffusion of atmospheric pollutants and the wind loading and wind flutter of buildings. From a single application's point of view, for the simulation experiments of the diffusion of atmospheric pollutants, the wind speed of the wind tunnel is approximately 0.1 m/s-10 m/s (or 15 m/s). However, the wind loading and wind flutter building model experiments require the wind speed to be in the range of 8 m/s-40 m/s. For the point of view of multiple purpose applications, the wind speed range will have to be extended to between 0.1 m/s-30 m/s if both requirements are to be satisfied simultaneously. From the viewpoint of design and utilization, in a single purpose wind tunnel, because of its small wind speed range, it is easier to manage its fan power system. Even so, for a wind tunnel designed for atmospheric diffusion, the wind speed varies from 0.1 m/s

to 10 m/s. Its magnitude differs by a factor of 100. It is difficult to materialize by relying on a silicon controller alone. It will have to be complemented by a change of fan moment. The number of fan blades had better be over eight. Because it is necessary to reach the extremely low wind speed, the revolution of the electric motor must be reduced to approximately 100 rev/min. Under such conditions, it will cause flow impulses if the number of blades is small which will affect the flow quality in the experimental section. Obviously, it is costly to design and construct such a variable moment fan. If the requirements can be lowered, then the present helicopter fan system can be slightly modified. Thus, it is only possible to have 3-4 blades. For example, the wind tunnel at the Environmental Protection Agency of the U. S. has a five blade variable moment axial flow fan
system. The maximum fan revolution speed is 900r · p · m ($v = 8$m/s), 22
and the minimum fan revolution speed is 20r · p · m($v = 0.15$m/s).

For a wind tunnel, specially for the testing of wind loading and wind flutter of buildings, the wind speed range is small (the magnitude differs by 8-10 times). It will be satisfactory to use a silicon controller to adjust the speed.

If a multiple purpose wind tunnel is to be constructed, for instance, the wind speed range is 0.1 m/s-30 m/s with a wind speed ratio of 300, we must solve the problem of continuous speed variation for such a large wind speed range. If no other method is available, we will have to combine the use of a silicon controller and a variable moment fan to adjust the speed. For example, the micro-meteorological wind tunnel at Colorado State University in the U.S. adopted a four blade variable moment fan system. Its wind speed range is 0.1 m/s-37 m/s.

The cross-sections of the test sections of most of the environmental wind tunnels are square or rectangular. Due to the secondary flow effect of the square cross-section, the effective experimental zone will be affected. Furthermore, a square cross-section is not very ideal for experiments on the study of a large scale pollutant diffusion, the effect of surrounding terrain on the buildings and an architectural group. Hence, the width to height ratio of the cross-section in the experimental segment must at least be 10:7 or 2:1. For an environmental wind tunnel, the key problem is the thickness of the simulated atmospheric boundary layer. Usually, in order to solve most of the problems in production, the simulated atmospheric boundary layer thickness must be at least δ — 1m or even larger. The actual atmospheric boundary layer thickness is between 500 m to 1000 m. Thus, the model is reduced at a ratio of about 1/500-1/1000. The height of the experimental segment must be approximately 2m. The width of the experimental section must depend on the range of terrain to be simulated. The large size environmental wind tunnel at the Japanese Pollution Research Institute, 10 m x 2.5 m x 30 m (direct blow type), has been used to simulate a 40 km wide range of terrain around Tokyo. The reduction ratio of the model was 1/4000. Due to its geographic location, the Boashen Steel Factory near Shanghai may cause pollution to Shanghai. If the affected area is considered to be 10 km wide and 20 km long, the reduction ratio will be about 1/3300 by using 3 m x 2 m cross-section experimental segment wind tunnel for a model test. The experimental tail flow zone length will have to be about 6 m.

For an environmental wind tunnel, if the study of atmospheric pollution diffusion is its main objective, then the simulated temperature layer structure is a key problem. For a wind tunnel with a 1.5 m x 1 m cross-sectional experimental section, in order to simulate the various environmental flows under different stable and unstable conditions and also to ensure a fixed Reynolds' number range, the maximum temperature difference of the temperature section should be at least about 80-100°C. Thus, it is required to have a heated or cooled ambient temperature of 5-90°C and a heated or cooled base plate temperature at 5-180°C. When the wind speed is 1 m/s, the power needed to carry out an experiment with a temperature layer structure is about 300-400 kw. If the cross-section of the experimental section of the wind tunnel is 3 m x 2 m and the wind speed is 1 m/s, the power required to obtain the same order of magnitude of temperature difference will have to be above 1200 kw-1600 kw (not including the electrical power consumed by the fan power system). Therefore, for a wind tunnel

constructed for the study of atmospheric pollutant diffusion, the selection of its cross-sectional dimension is a problem to be thoroughly considered. Of course, there are still many large environmental wind tunnels with temperature layer structures in the world. For example, a circular flow wind tunnel in France has an 8 m x 3 m x 40 m cross-sectional size and the base plate temperature is 10-70°C. A direct blow type of wind tunnel at the Japanese Pollution Research 23
Institute has a 10 m x 2.5 m x 30 m size test section. It is also equipped with a temperature gradient and a turbulence generator. For a wind tunnel this size, the amount of electricity consumed is significant.

As for the problem of the selection of the length of the test section, some wind tunnels have a test section length of longer than 24 m. Some of them are slightly shorter which is about six times the height of the cross-section. Based on the artificial boundary layer formation method, using the 1/4 elliptical whirlpool generator method as an example, it is possible to form the required velocity section within a short distance from the inlet of the test section. For a wind tunnel with an experimental segment cross-section of 3 m x 2 m, in order to form a 1 m thick atmospheric layer the height of the 1/4 elliptical generator should also be about 1 m. At about 3 m-4.5 m behind the generator, the required velocity section is formed. Together with the tail flow region of the model of 4 m-5 m, the length of the experimental section will have to be about 10 m. For the artifically formed atmospheric layer using the injection method, a longer test section is required. If we use a 3 m x 2 m cross-section experimental segment as an example, the length of the experimental segment will have to be about 15 m. We can see that the length of a short test section environmental wind tunnel is about half that of a long test section wind tunnel. From the angle of reliability, it is always better to build a long test section. It is especially true for an environment wind tunnel with a temperature layer structure. Obviously, if we want to build a larger experimental wind tunnel for the wind load and wind flutter testing of buildings, then we should consider a test section with a shorter artificially formed boundary layer.

In summary, the selection of the length of the test section should be based on the result obtained after considering all the factors.

As for the wind tunnel type problem, there are approximately three types. One of them is the circular type of wind tunnel (or they can be converted into the direct flow bending type). The micro-meteorological wind tunnel at Colorado State University in the U. S. can be used as an example of this type of wind tunnel. It is usually controlled by a single axial fan which has a variable moment. This arrangement would significantly extend the range of wind speed. When a high wind speed (above 30 m/s) is used to conduct an experiment on wind load and wind flutter of building, it can be used as a circular type of wind tunnel. In this case, the energy of this wind tunnel is comparatively high to sufficiently utilize the capability of the power system. When it is used in an atmospheric pollutant diffusion experiment which is conducted at a low wind speed (0.1 m/s-5 m/s), the circular flow is changed to a direct flow bending type. At this time, the effect of external flow on the flow field in the test section is comparatively small for a direct flow wind tunnel. The amount of energy retrieved from the circular flow channel in a circular wind tunnel is only a few percent of the total energy. Its main function is to make the flow entering the stable section uniform without the effect of gust. Furthermore, if a temperature layer structure exists, the heating of the ambient temperature is placed in front of the third turn. Thus, the ambient temperature can be controlled with uniform stability to a certain extent. Of course, its building cost is 70%-100% higher than that of a direct flow wind tunnel with similar characteristics. The second type is a direct flow section wind tunnel. Usually, there is one (or more) axial flow fan downstream from the test section. For example, the wind tunnel of US EPA (its test section dimensions are 3.7 m x 2.1 m and its test section length is 18.3 m) belongs to this type. The pressure in the test section is less than the external pressure for this type of wind tunnel in low speed testing, gas would leak from the outside in when the wind tunnel is operating. This may affect the flow quality of the test section. Therefore, the requirement of wind tunnel body hermeticity is comparatively high. The inlet and outlet of a direct flow wind tunnel are the necessary path for an external gust to affect the dynamic pressure of the test section. Hence, it must be treated with special caution. By installing flow guiding devices and fine nylon nets at the wind tunnel inlet and a few parts in the tunnel body, the effect of gust is reduced to the extent possible. The dust brought in by the external flow may have some deterimental effect on the probe of the thermal linear wind speedometer. Therefore, it is necessary to frequently wash the nylon mesh. The room with the wind tunnel must be kept clean. The inlet and outlet of the wind tunnel should have air filters installed. A 3-4 layer mesh is used at the inlet and a double layer mesh at the outlet having the function of adjusting and stabilizing the flow. However, the installation of more flow control meshes will consume more power (approximately 15%). In addition, for a direct flow wind tunnel, its noise is larger. It is especially true at high wind speeds. The noise of a direct flow wind tunnel includes the noise generated by the fan itself and the noise caused by the vibration of the body. This not only would interfere with the thermal linear probe, but also would affect the turbulence of the flow. It should be eliminated by taking the proper measures. In the fan section of the wind tunnel in the U.S. EPA used a series sound proofing measures to minimize the effect of noise to the fullest extent possible. If a direct flow wind tunnel is built indoors, the building itself forms a back loop. Thus, it is possible to carry out a certain control with respect to temperature. Furthermore, the effect of external gust is also reduced. However, as a wind tunnel for use in atmospheric pollutant diffusion, its fume must be led to the outside. Otherwise, the concentration of the smoke itself will be affected if it is circulated in the room before entering the inlet of the wind tunnel. The third one is the direct flow blowing type wind tunnel such as the one at the Japanese Pollution Research Institute which is 10 m x 2.5 m x 30 m. This type of wind tunnel has a fan upstream from the stability section. It is more advantageous to use a centrifugal fan, especially under conditions not originally designed for. The use of a centrifugal fan can produce a larger pressure rise. In addition, the whirlpool at the outlet is comparatively small. The pressure in the experimental section of this type of wind tunnel is larger than that of the outside. During operation, gas leaks from inside out. The effect on the flow in the test section is not too large. The requirements of seals for the wind tunnel body can be relaxed. Obviously, the treatment of the inlet and outlet of a wind tunnel is similarly very important. In the design of Japanese environmental wind tunnels, most of them used the direct flow blowing type, especially when the wind speed range is 0.1 m/s-10 m/s. It is more advantageous to adopt this form under this condition.

AERODYNAMIC COMPUTATION OF THE WING--BODY--SHORT CABIN COMPOSITE* 39

Chen Yao Song
(Department of Mechanics, Beijing University)

1. INTRODUCTION

The aerodynamic computation of an airplane including the wing--body and short cabin is a large topic. In the subsonic and supersonic regions, the finite basic solution is commonly considered as the best method to solve the ideal potential flow [1]. Because the requirements
for aerodynamic computation are becoming higher and higher, the dis- 40
cretization of the aircraft surface is getting finer. Therefore, the internal storage must be greater. The computational work load is also increased. In order to resolve the difference between supply and demand, presently we still rely on the partial computation with the perturbation method. Due to the mutual dependence between the partial aerodynamic force and perturbation, repeated iterational computation is unavoidable. Furthermore, the actual partial method has a determining effect on the convergence property and speed of iteration. When the treatment is improper, the computation will fail. In this paper, a method to extract the "perturbation" was designed. It can completely avoid iteration so that the required internal storage is reduced and the computational work load is decreased. Currently, some

*Received on May 26, 1980

factors, such as the thickness and curvature of the wing, are separated first to simplify the computation. But the computation of the two factors can be done separately. The results obtained first can be used to refine the presentation of the boundary condition of the latter computation. By doing so, the work load is not increased but the final results are greatly improved.

II. EXTRACTION OF AERODYNAMIC PERTURBATION

Using the aerodynamic interference of a wing on a body as an example, it is required to find the added flow field on the wing produced by the basic solution of the body. However, Q_B itself is required to be determined simultaneously with the basic solution Q_W of the wing. If the same block method is used to find the perturbation field of the body to the wing and the induction field of the body itself (Figure 1), the order of the simultaneously obtained equations is very high. If different methods are used for both cases now in the computation of mutual perturbation between the wing and the body, very small size blocks are reserved for the area near the wing-body connection. The block size is amplified in the areas where they are far apart. (From a simple analysis, we know that the linear dimension of the block is proportional to the distance between perturbed points. It increases accordingly. Therefore, the relative error introduced by discretization still remains on the same order of magnitude). Consequently, the number of unknowns to be solved simultaneously is greatly reduced. By independently solving such a wing-body composite to obtain Q_B' and Q_W', it is possible to obtain the perturbation fields of body on wing and wing on body (Figures 3 and 4), respectively. This perturbation field is computed in one computation. With it, the aerodynamic force on the wing or body can be calculated independently. In this case, the blocks are divided separately. Generally, the blocks are getting smaller (its size is equivalent to the smallest block used in the computation of the perturbation).

III. DECOMPOSITION OF THE BOUNDARY CONDITION AND THE COMPUTATIONAL SEQUENCE

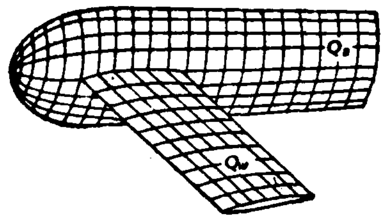

Figure 1

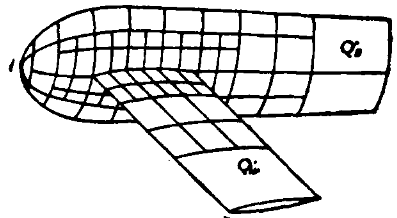

Figure 2

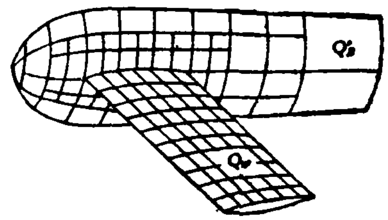

Figure 3

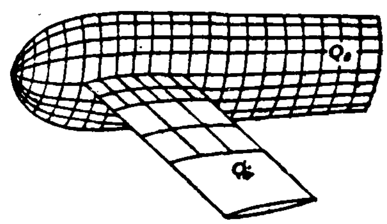

Figure 4

The circular flow condition on the surface of an object can usually be written as

$$(\boldsymbol{v}_\infty + \boldsymbol{v}) \cdot \boldsymbol{n} = 0 \qquad (1)$$

where $\boldsymbol{v}_\infty$ is the velocity of incoming flow, $\boldsymbol{v}$ is the perturbation velocity, $\boldsymbol{n}$ is the unit normal vector on the surface of an object (see Figure 5). As far as the wing is concerned, this condition can be simplified somewhat. Let u, v, w and n_x, n_y, n_z be the three components of $\boldsymbol{v}$ and $\boldsymbol{n}$, respectively. On a normal wing, $n_y \ll 1$. Therefore, on the wing, it is approximately

$$n_x \cdot u + n_z \cdot w = -(v_{\infty x} \cdot n_x + v_{\infty z} \cdot n_z) \qquad (2)$$

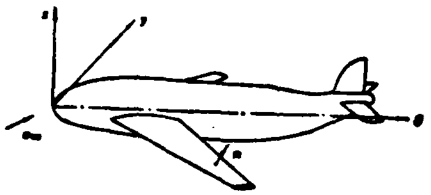

Figure 5

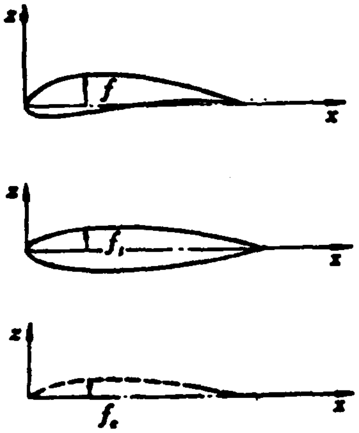

Figure 6

where $v_{\infty x}$ and $v_{\infty z}$ are the x and z direction components of the incoming flow velocity v_∞ . If the wing shape is given in a function form

$$z = f(x, y) \tag{3}$$

then equation (2) can be written as

$$\frac{v_{\infty z} + w}{v_{\infty x} + u} = \frac{\partial f}{\partial x} \tag{4}$$ 41

Assuming that the attack angle of the incoming flow is α and f_t and f_c are the wing thickness and curvature, respectively (Figure 6), if the incoming flow velocity is equal to 1, then the wing condition (4) can be written as

$$\frac{\sin\alpha + w}{\cos\alpha + u} = \frac{\partial f_c}{\partial x} \pm \frac{\partial f_t}{\partial x} \tag{5}$$

In the actual computation, we usually have to perform the following simplification:

1. The circular flow condition (5) to be satisfied originally on the wing surface (z = f) is shifted to the chord plane (z = 0).

2. It is believed that $|u| \ll \cos\alpha$, is valid everywhere on the wing surface so that u can be omitted in the formula.

When the curvature and thickness of the wing are not large and the attack angle is small, this kind of simplification is permitted. However, we should point out that the u near the front fringe is on the same order of magnitude as cos α. Therefore, the solution obtained after such a simplification would not be too good near the front fringe of the wing. In order to improve this point, we are temporarily abandoning the second point of simplification. In this case, the circular flow condition becomes

$$w = \pm(\cos\alpha + u)\frac{\partial f_t}{\partial x} \qquad + (\cos\alpha + u)\frac{\partial f_c}{\partial x} - \sin\alpha \tag{6}$$

Let us break it down into two parts

$$w = w_t + w_c \tag{7}$$

where

$$w_t = \pm(\cos\alpha + u)\frac{\partial f_t}{\partial x} \tag{8}$$

$$w_c = (\cos\alpha + u)\frac{\partial f_c}{\partial x} - \sin\alpha \tag{9}$$

If the solution φ_t and φ_c, under the conditions $w = w_t$ and $w = w_c$ can be obtained by iteration, then they are the solutions to the thickness and lift problems, respectively. As a first order approximation, let us simplify the condition (8) of the thickness problem as

$$w_t = \pm\frac{\partial f_t}{\partial x} \tag{10}$$

Because everything on the right side is known, the corresponding solution φ_t can be directly obtained from the method of placing a planar source on the chord plane. After finding φ_t , it can be substituted into the circular flow condition (9) of the lift problem:

$$w_c = \left(\cos\alpha + \frac{\partial \varphi_t}{\partial x}\right)\frac{\partial f_c}{\partial x} - \sin\alpha \tag{11}$$

The corresponding solution φ_c can be obtained by using the method to arrange the equal pressure surface vortex by the division of blocks on the chord plane [2]. By calculating according to the sequence mentioned above, we can obtain better results without iteration.

The above is basically the Woodward method. The only difference is that after solving the thickness problem, the results obtained are used to correct the boundary condition of the curvature problem. In the final computation of pressure, the nonlinear terms of the incoming flow direction velocity component are maintained. By doing so, the computational work load is not increased as compared to that of the Woodward method. However, the results, especially the results near the front fringe, agree with the experiments more satisfactorily (the difference is reduced by half on the average). Therefore, in the computation of the composite structure, we also carried it out accordingly.

As for the boundary condition of the wing of the composite body, it is still to be satisfied by shifting to the wing chord plane. On the projection of the chord plane of the wing, blocks are evenly divided. Each block is arranged to have a linear planar source with a strength yet to be determined and an isobaric surface vortex. Due to that fact $n_y \ll 1$, the effect of the lateral sliding velocity component can be neglected. This means that it is possible to only consider the velocity components u and w where we establish the boundary condition of the wing. Assuming that the wing thickness part is $f_t(x,y)$ and the curvature part is $f_c(x,y)$, then the velocity field created by the planar surface arranged on the wing surface is (u_t, w_t) and the velocity field created by the arranged surface vortex is (u_c, w_c). Because a composite body is studied, we must also consider 42
the existence of the body and the short cabin. Blocks are also drawn on their surfaces. A uniform planar source is arranged and control points to establish the boundary conditions are established [3]. The velocity field created by these planar sources near the wing is called (u_h, w_h).

Now, let us study the uniform flow from the x-direction (1,0). Then the velocity field on the wing (u,w) can be written as

$$\left.\begin{aligned} u &= 1 + u_h + u_t \pm u_c \\ w &= w_h \pm w_t + w_c \end{aligned}\right\} \qquad (12)$$

where the top signs represent the flow field on the top surface of the wing and the lower signs represent the flow field on the lower surface of the wing. The normal directions of the top and bottom wing surfaces (n_x, n_z) can be replaced by the directional numbers $(-f'_c \mp f'_t, 1)$ where $f'_c = \frac{\partial f_c}{\partial x}$, $f'_t = \frac{\partial f_t}{\partial x}$. Therefore, the boundary condition on the wing can be written as

$$-(f'_c \pm f'_t)\cdot(1 + u_h + u_t \pm u_c) + w_h \pm w_t + w_c = 0$$

i.e.,

$$[f'_c\cdot(1 + u_h + u_t) + f'_t\cdot u_c - w_h - w_c] \pm [f'_t\cdot(1 + u_h + u_t) + f'_c\cdot u_c - w_t] = 0 \qquad (13)$$

Originally, they should be satisfied on the top and bottom surfaces, respectively. However, according to the experience in the computation of the single wing, we can make the contents in the two brackets zero individually to form two boundary conditions

$$f_t' \cdot (1 + u_b + u_t) + f_c' \cdot u_c - w_t = 0 \tag{14}$$

and

$$\begin{aligned} f_c' \cdot (1 + u_b + u_t) + f_t' \\ \cdot u_c - w_b - w_c = 0 \end{aligned} \tag{15}$$

In the real aircraft, the blocks on the body and the short cabin near the wing have a weaker source converging strength because they are close to the incoming flow direction. Thus, one can assume that

$$u_t, u_c, u_b \sim O(\varepsilon) \tag{16}$$

Here, ε is a small quantity representing the order of magnitude of the attack angle α as well as f_c' and f_t'. Therefore, we can adopt the following form of wing boundary conditions:

$$w_t = f_t' \tag{17}$$

$$\begin{aligned} (w_b - u_b \cdot f_c') + (w_c - u_c \cdot f_t') \\ = (1 + u_t) \cdot f_c' \end{aligned} \tag{18}$$

In equation (17), all the higher order terms have been eliminated. The distribution of the planar source can be directly determined by f_t. But the boundary condition (18) is used after the thickness problem is solved. Therefore, it is possible to keep $u_t \cdot f_c'$ as an unknown term on the right side of the equation.

Now, let us analyze the circular flow problem of the unity parallel flow along the z-direction (0,1). In this case, equation (12) can be written as

$$\left.\begin{aligned} u &= u_b + u_t \pm u_c \\ w &= 1 + w_b \pm w_t + w_c \end{aligned}\right\} \tag{19}$$

Corresponding to equations (14) and (15), there are boundary conditions as follows:

$$f_t' \cdot (u_b + u_t) + f_c' \cdot u_c - w_t = 0 \tag{20}$$

and

$$\begin{aligned} f_c' \cdot (u_b + u_t) + f_t' \cdot u_c - 1 \\ - w_b - w_c = 0 \end{aligned} \tag{21}$$

Different from the condition of parallel incoming flow, now the wing has

$$u_c, w_c, u_h, w_h \sim O(1) \tag{22}$$

and

$$u_t, w_t \sim O(\varepsilon) \tag{23}$$

After neglecting the higher order terms of $u_t \cdot f_t'$ and $u_t \cdot f_c'$ in equations (20) and (21), respectively, the two boundary conditions can be written as

$$w_t = u_c \cdot f_t' + u_h \cdot f_t' \tag{24}$$

and

$$(w_h - u_h \cdot f_c') + (w_c - u_c \cdot f_c') = -1 \tag{25}$$

For a perpendicular flow problem, the plane source of the short cabin on the body and the surface vortex of the wing can be solved by equation (25) first. Then, equation (24) can be used to solve the plane source problem of the wing.

As for the boundary conditions on the short cabin or the body, for parallel incoming flow, we have

$$(u_h + u_c) \cdot n = -u_z - u_t \cdot n \tag{26}$$

But for perpendicular flow, because u_t is one order higher than u_h and u_c, we can neglect the $u_t \cdot n$ term so that it becomes

$$(u_h + u_c) \cdot n = -u_z \tag{27}$$

Because in the perpendicular circular flow problem the solving of the wing surface source comes after solving for the wing surface vortex and body (or short cabin) plane source, this omission becomes necessary. Otherwise, the three equations must be solved simultaneously and the problem becomes immense again.

In summary, f_t' is used to solve the wing surface source problem with parallel flow. Then, the expansion matrix is used to simultaneously solve the wing surface vortex and the surface source of a short cabin or body problems with parallel and vertical flows. If the only thing required is the aerodynamic force on the wing surface, then the last step can be skipped. This is because the perturbation source only comes from the surface source on the short cabin or the body.

IV. EXAMPLE 43

After proposing the above algorithm, actual computations were carried out using the DJS-18 computer at Beijing University based on the domestic "transport light" aircraft. The blocks of the body, wing and short cabin are shown in Figures 7, 8 and 9. Figure 10 is the lateral distribution of the wing rotational moment c-C_L curve when the attack angle is 4°. Because the short cabin has a -4° installation angle with respect to the wing, therefore, the consequence of short cabin interference is the reduction of lift. This is extremely serious when the attack angle is small. It decreases with increasing attack angle. Near the short cabin, the reduction of the circular moment agrees with the experimental results. The circular moment curve obtained by the computation indicates that the lift coefficient when $M = 0.6$ is about 20% larger than that at $M = 0$. Because there is no experimental result at $M = 0.6$, we can only compare our results to the calculated results by sombody else [4]. It is also reasonable.

When using an aerodynamic perturbation method to calculate the aerodynamic force of a composite body, the most serious test is to determine whether the local aerodynamic force distribution is reasonable at the junction between parts. In Figure 11, the pressure distributions on the top surface in the chord direction of the wing with $y/L = 26.2\%$ and 83.8% are plotted. The latter is far from the body and the short cabin which is a typical top surface pressure distribution on a single airplane wing, while the former happens to be on the top of the inner side of the short cabin. As for the effect of the short cabin on the upper wing surface pressure distribution, besides the occurrence of some fluctuations locally at the front fringe, in the large area it tends to even out the pressure. It is also reasonable.

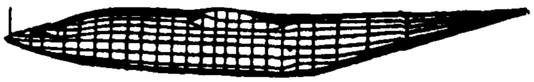

Figure 7

Figure 8

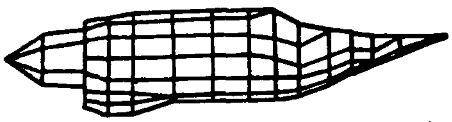

Figure 9

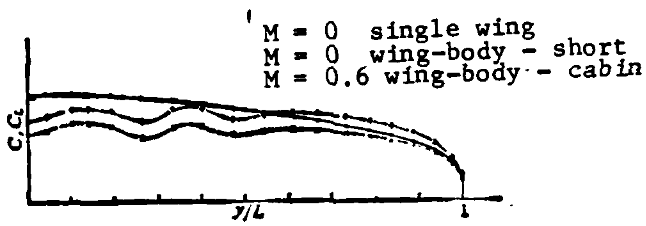

Figure 10

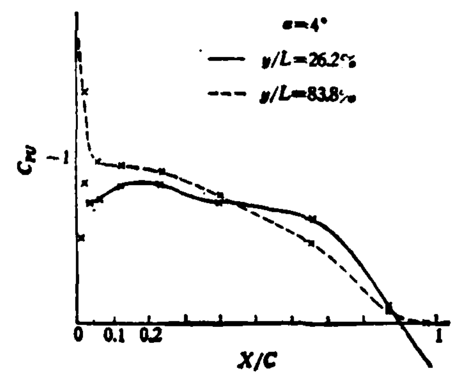

Figure 11

All in all, actual computation indicates that it is feasible to realize the computation of a composite body by using the "perturbation extraction method". In this case, the capacity of the computer required is less which is very meaningful.

NOTICE OF NAME CHANGE FOR "Electronics Communication".

"Electronics Communication" will change its name to "Journal of Electronic Science" in 1983. It will remain to be a technical publication. We welcome your manuscripts and your subscriptions also.

REFERENCES

[1] Wirz H. J., Smolderen, J. J., Numerical methods in Fluid Dynamics, McGraw-Hill Co., Chapter 4 (1978).

[2] Woodward, F. A., An Improved Method for the Aerodynamic Analysis of Wing-Body-Tail Configurations in Subsonic and Supersonic Flow, NASA CR-2228 (1973).

[3] Hess, J. L., Calculation of Potential Flow about Arbitrary Three-dimensional Lifting Bodies, MDC J5679-01. final report (1972).

[4] Ferrari, C., Interaction Problems. High Speed Aerodynamics and Jet Propolsion. VII. part C, Princeton Univ. Press (1957).

The "Optical Oil Flow" Technique in a shock wave wind tunnel

In a piece of equipment such as an equal impulse shock wave wind tunnel, the display of the flowing motion often relies on the printing (shadow) method. However, the oil flow technique, which has been widely used in conventional wind tunnels, is not applied in this area maturely. Up until now, in the relevant information both domestically and abroad, there is very little successful application being reported using this technique for an impulse type wind tunnel.

The aerodynamic center carried out an experimental study on the "optical-oil flow" display technique in a shock wave wind tunnel. This wind tunnel has conical nozzles. There are observation windows on both sides of the test section. The diameter is ϕ 240 mm. The experimental model is a plate-cylinder composite body. The body was installed on the symmetry plane in the test section in an attitude approximately perpendicular to the horizontal plane. The attack angle is $\alpha \approx 3°$. The M number of the flow at the outlet of the nozzle is close to 8. It could also ensure the presence of a turbulent surface layer on the plate in front of the cylinder. The experimental time period is approximately 7 milliseconds. Obviously, the extremely short experimental period is the major reason making it difficult to apply the oil flow technique. After taking the corresponding measures, we have successfully obtained clear flow pattern photographs (photographs 1 and 2) related to the supersonic turbulent surface layer separation in front and behind the cylinder. From these photographs, we can obtain the knowledge regarding the separation of supersonic turbulent surface layers in front and behind the cylinder.

It should also be pointed out here that: The current flow pattern photograph is not taken after the experiment. Instead, it is taken during the experimental (blowing) period after the flow field has already been established. The results obtained experimentally showed that the flow pattern in the testing process is quite different from

Figure 1

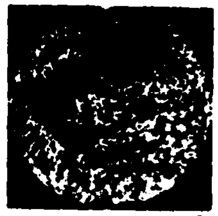

Figure 2

that after the experiment. This not only indicated that the stopping of the wind tunnel has a significant effect on the flow pattern, but also demonstrated that the current oil flow technique has the capability of reflecting the flow variation correspondingly. Other experiments also demonstrated that the present oil flow technique has sufficient capability to reflect a uniform flow pattern.

The use of an optical method is an important means of flow display in wind tunnel experiments. The "optical oil flow" technique combines the oil flow technology with a certain optical technology. It can correspondingly improve the resolution of surface flow lines. It is also able to record the position of the shock wave. This technique has been used in shock wave wind tunnels. It is anticipated to extend it to other millisecond level impulse type wind tunnels.

Yang Zuqing and Wang Xirong

The photographic technique of shock wave laser shadow

When an aircraft is in a supersonic flow, it collides with natural and artificial solid and liquid particles. The bow shaped shock wave is distorted and the heat flow is increased significantly. However, due to the fact that the shock wave distortion is random, its position and direction do not follow a certain law. The deflection of high velocity particles will cause the occurrence of shock wave oscillations. Therefore, it is comparatively more difficult to photograph the high speed shock wave distortion. Presently, the 701 of the 7th Machinery Department uses a pulsed laser high speed shadow technique to obtain better results. The shadow method can reflect the variation of the flow in any direction. The light source used was a pulsed ruby laser with chlorophyll D to adjust Q. The pulse width can be under 100 ns. Because of the better monochromatism of the laser, the sensitivity is higher. As long as the area of the point light source is small and there is a proper distance between the flow disturbance to the base plate, we can get better photographs. The shadow method does not need a knife edge it can prevent the light diffraction effect created by the knife edge in the grain method. The image formed is very clear.

In order to study the mechanism of erosion and corrosion of the aircraft due to these particles, not only do we need to observe the distortion of the bow-shaped shock wave, but also simultaneously we wish to obtain the information on the size and density distribution of the high speed particles. Therefore, the use of an axial holographic photographic method is a better method to study microscopic dynamic particles. It not only can display the three-dimensional picture of the original particle field to obtain the relevant data on the size and distribution of particles, but also can simultaneously observe the shadow diagram of the bow-shaped shock wave distortion.

Yuan Ge, Jin Yuan and Li Chaojie

The fluidized pressure transfer equipment for powdered coal

Coal fixed magnetohydrodynamic generation of electricity is a power generation method which uses the high temperature high velocity plasma flow ($T \approx 3000°K, M \approx 1$) produced by having powdered coal pass through a magnetic field while cutting the magnetic line of force to generate electricity. Presently, some countries in the world are very serious about this study. In order to adapt to the requirements of this study, the Electrical Engineering Institute of the Chinese Academy of Science constructed a simple fluidized pressure transfer device for powdered coal in October 1980. A cold state test was conducted. Furthermore, several tests of electricity generation were performed in 1980 and 1981. The operating condition showed that the transfer concentration of the device (the ratio of the transferred powdered coal vs. the carrier gas by weight) could be adjusted in the range of 30-500. The flow rate could vary in the range from 80-300 g/sec. During stable operation, the fluctuation of the flow rate of the powdered coal does not exceed ±10%. It might be because since the experimental range was limited, the relation between the flow rate and the pressure of the coal can was close to linear. In addition, preliminary explorations with regard to the correlations between the fluidized gas, transfer gas and powdered coal flow rate were conducted.

The structure of this device is as shown in the figure. In the figure, the gas line I is the pressurizing line. A certain pressure is maintained in the powdered coal can through adjusting the gas flow rate in that line. II is the fluidizing gas line. The gas is blown into the top of the powdered coal can by passing through the fluidization plate in the fluidization chamber to fluidize the powdered coal. The fluidized bed used was the flat bottom plate type. III is the transfer gas line. The gas is injected into the coal mixer through the acceleration at the gas nozzle to cause the further fluidization. This equipment did not use a mechanical material supply device because we had wished to control the flow rate of powdered coal by controlling the gas flow parameters. An explosion proof diaphragm was installed on the powdered coal can to ensure safety. The inner diameter of the coal can is ϕ 600. The flow rate of the coal powder was measured by the pound. The gas flow rates were measured using three separate gas rotor type flow meters.

On the basis of this device, the institute is currently building an optical grating type of electronic scale for weighing. It will be used in a larger scale fluidized pressure transfer device for powdered coal to automatically adjust and control the operation continuously. By that time, we should be able to conduct more thorough tests.

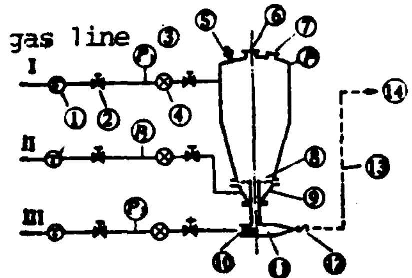

Schematic diagram of the
coal transfer device

1--reducing valve; 2--needle valve; 3--pressure gauge; 4--float type flow meter; 5--release valve; 6--coal entering hole; 7--explosion-proof hole; 8--fluidized plate; 9--fluidized chamber; 10--gas nozzle; 11--mixer; 12--manual valve; 13--coal transfer tube; 14--to the combustion chamber

Dong Chengkang and Zhang Guichun

The free surface shock wave in the near field of ships

In recent years, an interesting characteristic of the ship wave was discovered in ship model experiments. There is a wave series which is completely different from the Kelvin series in the wave pattern of the near field of a ship. It looks like the shock wave of a compressible fluid. Therefore, it is called the free surface shock wave. The free surface shock wave (non-linear wave) and the Kelvin wave (linear wave) exist simultaneously near the hull of a ship. The free surface shock wave occurs in the near field of a ship while the Kelvin wave appears at a certain distance from the ship.

The so-called shock wave is characterized by the presence of a discontinuous flow surface. The velocity varies abruptly before and after the shock wave. According to the measurement of velocity distribution in the ship near field (the bow and the stern), the perturbation velocity component (ν) in the transverse direction (y) and the wave height (ζ) have a step effect, as shown in Figure 1. This type of step jump effect is limited to a thin layer near the free surface.

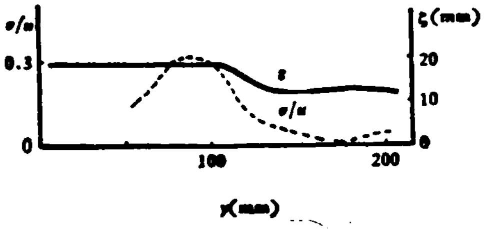

Figure 1

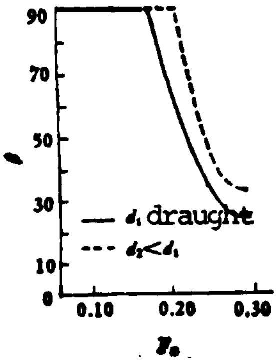

Figure 2

Just because of these reasons, some people suggested that it should be called the free surface shock wave. Furthermore, it was believed that a nonlinear shallow water wave could be used to analyze this type of shock wave effect. After introducing an equivalent draught $\bar{h}$, the correlation curve, as the one shown in Figure 2, was discovered between the shock wave angle of the free surface β (the angle between the wave front and the direction of sailing) and the Flute number F_n of the ship length. When the shock wave angle is 90°, it is called a normal shock wave. When the shock wave angle decreases rapidly with increasing F_n, it is called the slanted shock wave. It resembles very closely the variation of Mach angle in a supersonic flow, i.e.,

$$\sin\beta = \frac{C}{U}$$

where u is the speed of the ship and C is critical velocity of equivalent draught, i.e.,

$$C = \sqrt{g\bar{h}}$$

The discovery of the free surface shock wave phenomenon is currently promoting the further development of the theoretical study of the wave generating resistance of ships.

Wang Xianfu

Based on "Collected papers of Japanese Shipbuilding Society" 147, June (1980)

A new shock wave tube

The Physics Department of Lehigh University in the U. S. has developed a new pressure driven shock wave tube. This shock wave tube does not use a diaphragm structurally. It uses a spring ball valve instead. The inner diameter of the valve is 2.22 cm. It is connected axially to a rigid driving section which is 60 cm long and 2.22 cm in inner diameter. The operating lever of the valve is connected to a spring mechanism. When the ball valve is triggered, it changes from a completely closed state to a completely open state by rotating 90°.

The spring ball valve: The driving section device has successfully produced light emitting shock waves in three driven sections during testing. In the experiment, air, argon, xenon and hydrogen were used together as the driving gas. The driven sections are three pieces of 3 mm inner diameter upper tubes with a length/radius ratio greatly exceeding 1000. These tubes were bent into any shape (the radius of curvature is as small as 10 times that of the radius of the tube). Each end was equipped with an organic glass experimental section with a rectangular or circular cross-section. After each discharge, most of the driving gas will be retrieved at high pressure. The driven section will not have the pollution problem by the atmosphere and the fragment of the diaphragm. Therefore, it is only necessary to clean the experimental section after several tests. Because the shock tube has the above advantages of bendability, reappearance of shock wave and cleanness, therefore, it is very suitable for large scale wave spectral studies.

Kang Zhixiang

A new impulse device

When a high energy pulse laser illuminates on a solid target material, an impulse is frequently produced. Impulse is an important mechanical parameter. It is imperative to the analysis of the mechanism of laser destruction. According to its application characteristics, we developed a practical laser velocity measuring solid rotational moment impulse device. This device is simple in structure, easy to use and reliable.

The instrument is composed of a freely rotating rigid body structure, a He-Ne light source, a photoelectric diode and an oscilloscope.

For a rigid body rotating freely around a fixed axis, a diamond bearing for instrument use was installed on the rotating axis. It was adjusted until the rotational friction was reduced to the minimum extent possible. Two arms were extended from the rotating axis and targets were installed at the end of the arm.

In the middle of the rotating axis, a small hole was drilled through the center of the axis to allow the light from the He-Ne laser beam to pass through this small hole. The light happened to shine on the photoelectric diode. When the rotating axis travels by an angle
of π, the photoelectric diode would receive an optical-electrical 80
signal. The signal was sent to the light display to record the amount of time required for the rotating axis to travel an angle π. Due to air resistance, friction and other factors, the rotating speed is always decreasing. Using an attenuation law to correct the amount of time to rotate an angle π, this corrected time can be used to obtain the rotational speed more accurately.

When the laser beam is shining on a stationary target, the target begins to rotate due to the impulse. Once the rotational speed is measured, we can very conveniently calculate the impulse.

Wang Chun kui

The powdered charge injection type shock wave device

According to a report in the "Abstract of Papers in the 13th International Shock Wave Tube and Shock Wave Conference" (July 1981), the Space Research Center of York University in Canada added a powder charge injection device to a conventional pressure driven shock tube. Due to the consideration of the recurrence of shock waves, the injection of charge and the firing sequence are automatically controlled. Therefore, the entire shock tube device works according to the following: the charge is installed in a tube inside the stabilization box. Then, the stabilization box was evacuated. In addition, it is filled with some buffer gas which is flowing towards the working section of the shock tube. The shock tube is also evacuated before operation. The first step of operation is to blow the gunpowder into the stabilization box. After waiting for a while, the suspended fine particles produced enter the shock tube with the buffering gas. Finally, the pressure is rapidly reduced by the medium gas to shatter the diaphragm (under the sequential automatic control condition; actually there are two diaphragms). The lasting time in the entire process is not more than one minute. In the operating process, all the valves and pressure transducers are equipped with microswitches to prevent malfunctions to affect the operation of the shock tube. The control system is composed of solid state transistor--transistor logic circuit elements.

The powder charge injection device can also reduce the waste rate caused by human error to improve safety.

Kang Zhi xiang

Solar laser

W. Wayford, et al of the United States National Aeronautical and Space Administration (NASA) used simulated sunlight at 4 kwatt to excite a quartz laser tube filled with C_3F_7I vapor to make it emit a pulse laser light with a peak power of 5 watts. This accomplishment has rekindled the interest to directly convert sunlight into laser light. The present problem is that the laser medium using C_3F_7I can only utilize 1% of the entire solar spectrum, i.e., the light with a wavelength between 250-290 nm. Therefore, the efficiency is very low. The researchers at NASA have already located an arsenic iodide compound which can utilize 7% of the solar spectrum. However, such a laser has not been developed yet. The laser which can be directly excited by sunlight is considered to be used in propelling the spacecraft in low orbits to higher orbits. Or, it can be used to feed energy to spacecraft or space bases. We also do not eliminate the possible military application of destroying satellites. There is another application which involves the assistance of this kind of laser to transmit the solar energy in space to the ground. If microwaves are used to transmit this energy, then we must construct a 29 square mile receiver on the ground. If a laser beam is used, the ground receiver is about the size of a football field. Lastly, we must solve problem of laser propagation in space, especially the attenuation problem during propagation in the cloud and storm. The present work is merely the first step. However, the future seems bright.

Li Yuanheng

Based on Science News
119(24), 381 (1981).

Using the single beam laser scattered spot interference method to measure the thermal strain

The measurement of thermal strain of a structure is a technique of high degree of difficulty. This is because the device to measure the strain itself is also affected by temperature. The resistance strain plate is an obvious example. The resistance strain plate is influenced not only by strain, but also by temperature.

F. P. Chiang studied the use of a single beam laser scattered spot interference method to measure the instantaneous thermal strain field of a small area heated aluminum plate with very good results. A ruby laser was used to minimize the correlating effect between the hot air turbulence and the scattered spot. Consequently, high quality equal displacement patterns were obtained. The experimental results showed that it not only can be an instantaneously varying but also a stable thermal strain field.

Fu Yushou

Based on Applied Optics 19, 16 (1980).

Metal fatigue causing aircraft mishap

The Boeing 737 passenger plane belonging to the Far East Airlines of Taiwan suddenly crashed which caused huge losses. The passenger plane seriously disintegrated in air which is a mystery.

Through analytical studies, the experts believed that this incident is due to metal fatigue. The aircraft disintegrated seriously in midair which indicates that metal fatigue has occurred in many areas of the major structure. An unstable state was reached at one instance. This phenomenon happened possibly due to the explosion of an engine.

High pressure is produced when the engine is started and this pressure disappears when the engine is shut off. The engine produces a periodically negative load. If the time of usage is long and the number of landing and takeoff times is high, even for an aircraft which is well designed, it may explode due to metal fatigue.

If regular checking is carried out to discover the symptoms of early stage metal fatigue, we can avoid the accidents.

Fu Yu shou

Based on The World of Science, 11 (1981).

Film used to measure pressure

The Fuji Film Company of Japan developed a film which is capable of directly measuring the pressure value and pressure distribution. It is called "プレスケール" . This film can be adhered to the surface of the object to be measured. Then, the pressure is applied to leave a pattern of different color darkness.

In the past, when measuring the pressure value and pressure distribution of a plane, the following methods were used: (1) to fasten a strain plate on the object to measure the strain; (2) to use a force measuring device or a piezoelectric crystal to measure the pressure; (3) to use the pressure print on the red lead powder (trilead tetraoxide) or aluminum foil to determine the contact points; (4) to use a strain painting film to determine the strained parts. However, it is not possible to accurately determine the pressure distribution and pressure value.

But, by using the newly developed pressure measuring film made by Fuji Film, anybody can simply measure the pressure distribution and pressure values. Therefore, a new territory in pressure measurement technology has been opened.

Its advantages are that: (1) it is capable of measuring the pressure exerted on a body due to contact which cannot be measured before, such as the pressure between the gears; (2) the measured pressure distribution pattern is clear at a glance; (3) it is possible to measure the pressure values by using a special colorimeter to determine the color; (4) the pressure range able to be detected is 5 kg/cm^2-700 kg/cm^2; (5) the measured pressure distribution pattern can be saved over a long period of time.

Actual examples and its effect: (1) the measurement of pressure on the contact plane of the valve gate: Because it is possible to determine the pressure on the entire contact surface easily, therefore, it is capable of determining the machinery condition and leakage at the contact surface of the valve and the seat. When the rotating moment of the valve lever is different, the pressure on the contact surface is also different. Therefore, it is possible to choose the most proper moment. (2) The measurement of pressure in the draining of a stainless steel bathtub: It is possible to determine the uniformity of the impulsive pressure. We can determine the stability of the strength and thickness of the product. It can determine the machining accuracy required for the punching die. (3) The measurement of pressure between the rollers in a Xerox machine: It is possible to simply measure the radial ellipticity of the roller, the linearity of the roller and the tightness width.

Jin Zhexue

Translated from Journal of Japanese Mechanical Society, 84, 748 (1981).

Diesel engine high speed automobile

The speed of the automobile to be used for aerodynamic study by Volkswagen Company in Italy is 225 miles per hour. The cruising speed also reaches the maximum value. This type of automobile can reach a speed of 155 miles per hour in a circular truck testing ground. On the average, each gallon of diesel fuel can run the vehicle for 39 miles. Even when moving at 225 miles per hour, each gallon of diesel can run the vehicle for 18 miles.

The designer installed a turbine pressurizer on a six-cylinder diesel engine in a light weight civilian truck. In addition, the pistons are cooled. These improvements raised the power of the diesel engine from 75 horsepower to 173 horsepower.

The key to the attainment of high speed for the automobile is the change of the aerodynamic external appearance of the car. The following factors were considered during the design: the maintenance of directional stability, the elimination of flow separation in front of the automobile, the cooling of the engine to reduce energy loss and the reduction of mechanical friction.

The shell of the automobile has been tested in the wind tunnel for a year and a half. Its resistance coefficient is lowered to 0.15 while the resistance coefficient of the unimproved automobile was 0.42.

Liang Xizhi

Based on Design News, 3 (1981).

The windmill with "pendulums"

The new windmill developed by the aerodynamic expert M. C. Chen at the United Technologies Research Center in the United States has been in operation. It has begun to feed electricity into the electrical network in New Zealand. This windmill has two blades; each blade is over 4 meters long. When in rotation, they appear to be the propeller blades of a helicopter. The special feature of this windmill is that two heavy objects which resemble a pendulum were installed at the junctions between the blade and the axis. These heavy objects work as the centrifugal engine adjusters. The higher the wind speed, the faster the blades rotate and the farther the pendulum is swung away from the equilibrium point. The result of the swinging of the pendulum would decrease the angle of inclination of the blade. Thus, a higher efficiency can be obtained at higher wind speeds. This windmill was installed on a 15 meter high tower. When the wind speed is 20 m/sec, it is capable of generating 8 kw of electricity. Its development was inspired to a great extent by the design of the composite bearing rotor of the Sikorsky S-76 helicopter tailwing.

Li Yuan heng

Based on Popular Science 218 (5), 24 (1981).

A new method to calculate the supersonic non-steady aerodynamic force

The paper written by Wang Xianxin of the 6th Institute of the Aerodynamic Center entitled "A Method to Calculate the Supersonic Nonsteady Aerodynamic Force and its Application in Flutter Analysis" provided a better way to calculate the supersonic nonsteady aerodynamic force and to analyze the flutter of aircraft parts. This method was formed by combining the supersonic nonsteady piston theory and the steady conical flow theory. It extended the mutual interaction between points on the wing which were neglected by the piston theory to the nonsteady condition using the conical flow theory. In that paper, 330 flutter computations for 29 states in 10 wing examples with four different planar shapes were conducted to verify and improve this algorithm for the supersonic nonsteady aerodynamic force. In this paper, the calculated results were compared to the wind tunnel experiment results and the calculated results were also compared to the flutter analysis based on the piston theory. Results showed that this method is suited for supersonic flutter analysis. It has the advantages of high accuracy, less computation time, easy steps and simply complied program.

Correspondent of this journal

The test of using a high energy laser to destroy guided missiles

After many years of preparation, the test of using on board lasers to destroy guided missiles was carried by the United States on June 1, 1981. However, this test was not successful.

This experiment was carried out using the Air Force Airborne Laboratory on the Boeing NKC-135 aircraft. A 400 kw aerodynamic laser was used. This laser was constructed by the United Technologies Corporation. Hughes Aircraft Company provided the precision light beam aiming and target searching tracking device.

The purpose of this experiment is to destroy the infrared self guidance flow regulating mask of the infrared sensor of the sidewinder missile because this is the weakest part of the missile.

The U. S. Air Force is currently checking for the causes of failure in order to determine the mode of failure. Further experiments will continue.

Fu Yushou

Based on AW & ST, [illegible], Jun.